Design of proton beam optics to realize beam distribution transformation in C-ADS HTBT *

WANG Xiang-Qi(王相綦)[1,3;1)] LUO Huan-Li(罗焕丽)[1,3] HAO Hao(郝浩)[1]
TANG Jing-Yu(唐靖宇)[1,2] LI Wei-Min(李为民)[1,3] XU Hong-Liang(徐宏亮)[1]

[1] National Synchrotron Radiation Lab., University of Science and Technology of China, Hefei 230029, China
[2] Institute of High Energy Physics, Chinese Academy of Sciences, Beijing 100049, China
[3] School of Nuclear Science and Technology, University of Science and Technology of China, Hefei 230029, China

Abstract: The linac to the transmuter beam transport line (LTBT) connecting the end of the linac to the spallation target is a critical sub-system in the accelerator driven system (ADS). It has the function of transporting the accelerated high power proton beam to the target with a beam footprint satisfying the special requirements of the minor actinide (MA) transmuter. In this paper, a preliminary conceptual design of the hurling magnet to transmuter beam transport section (HTBT), as a part of the LTBT, for the China ADS (C-ADS) system is proposed and developed. In this design, a novel hurling magnet with a two dimensional amplitude modulation (AM) of 1 kHz and scanning of more than 10 kHz at 360° in transverse directions is used to realize a 300 mm diameter uniform distribution of beam on target. The preliminary beam optics design of C-ADS HTBT optimized to minimize the beam loss on the vacuum chamber and the radiation damage caused by back-scattering neutrons will be reported.

Key words: C-ADS, LTBT, HTBT, hurling magnet, k-factor, double-waist

PACS: 29.27.Eg, 41.85.-p **DOI:** 10.1088/1674-1137/37/2/027004

1 Introduction

The accelerator driven system (ADS), first proposed in 1990s [1], is a promising solution to breed nuclear materials and transmutation of nuclear waste which are demanded and produced by the growing nuclear power industry. China-ADS (C-ADS) is a long-term project allocated by the central government aiming to build an industrial demonstration ADS facility in about 2032, and now it is in the R&D phase. The complex C-ADS assembly mainly consists of a high-power proton accelerator (HPPA) operating in continuous wave (CW) mode and a minor actinide (MA) transmuter. The sub-critical transmuter will be driven by the very high-flux neutrons produced in the process of the high-power proton beam bombarding the spallation target installed in the core of the transmuter. As an ultimate goal of the project, some main specifications of the C-ADS driver linac are listed in Table 1 [2–4].

In order to reduce thermal stresses on the proton beam window (PBW) which is used to separate regions from different vacuum conditions and the spallation target and to simultaneously improve the beam utilization, a particular beam distribution in these elements is desirable [5–8]. By considering C-ADS normal and safe operation, a uniformly distributed round beam with a 300 mm diameter integrated over a 1 ms time window in transverse directions is required as a preliminary design data of beam footprint on target, which maybe will be suitably adjusted in the future according to some further researches on the neutron dynamic of the transmuter.

Table 1. The main output specifications of the C-ADS driver linac.

parameter name	parameter value	unit
particle	Proton	
energy	1.5	GeV
current	10	mA
beam power	15	MW
frequency	162.5/325/650	MHz
duty factor	100	%
Norm. emittance (rms)	0.20	π mm·mrad
beam size (rms)	2.5 (1 $\sigma_{x,y}$)	mm
beam loss	<1 (or 0.3)	W/m
	<25000	1 s<t<10 s
beam trips/year	<2500	10 s<t<5 min
	<25	t>5 min

Some schemes of transforming the beam transverse distribution have been discussed, such as by using nonlin-

Received 23 April 2012
∗ Supported by National Natural Science Foundation of China (11045003, 10975150)
1) E-mail: wangxaqi@ustc.edu.cn

ear magnetic field [6, 9–11] or time-varying magnetic field [12–17]. Generally speaking, the transformation method using nonlinear magnetic field produced by a standard multipole magnet is conveniently used for the beam with a small emittance, but the circular beam distribution with a large radius on target is difficult to obtain. The transformation scheme using step-like nonlinear magnets [9, 10] is applicable for the beam with a large emittance to produce a parabolic-like or a fourth power-like beam. For time-varying magnetic field, beam distribution transformation would be carried out to date in such circumstances in which the angular and amplitude modulation frequencies are several tens Hz. For example, the angular and amplitude modulation frequencies in spiral wobbling method are 59 Hz and 23 Hz [16], respectively, and the horizontal and vertical angular frequencies in zigzag wobbling method 85 Hz and 23 Hz [17], respectively.

In this paper, the beam optics design of the hurling magnet to the transmuter beam transport section (HTBT), as a part of the linac to the transmuter beam transport line (LTBT) in C-ADS, is proposed by using a new type of AC dipole magnet, named hurling magnet, together with a specially designed beam transport line. Driven by a more than ten kHz sine-wave current with a 1 kHz amplitude modulation, the 6-pole hurling magnet can produce an amplitude modulated rotating dipole field, passing through which, the charged particle beam is scanned out in transverse directions. The beam optics of C-ADS HTBT is optimized for minimizing the beam loss and radiation damage caused by backscattering neutrons. Using the above scheme, a uniform round beam on the target can be realized for C-ADS.

2 The hurling magnet with a rotating dipole magnetic field

To obtain a uniform round beam on target, a rotating dipole magnetic field is considered. The dipole magnetic field rotates around the longitudinal axis of the transport line and is powered by sine-wave current with amplitude modulation (AM) in the form of Eq. (1)

$$f(t)=\begin{cases}\sqrt{4t/T_1-4n}, nT_1\leqslant t<nT_1+T_1/4\\ \sqrt{-4t/T_1+2+4n}, nT_1+T_1/4\leqslant t<nT_1+T_1/2\\ \sqrt{4t/T_1-2-4n}, nT_1+T_1/2\leqslant t<nT_1+3T_1/4\\ \sqrt{-4t/T_1+4+4n}, nT_1+3T_1/4\leqslant t<(n+1)T_1\end{cases}, \tag{1}$$

where T_1 is the AM period of the hurling magnet, and n is an integer.

The longitudinal spacing between two adjacent proton microbunches in C-ADS HTBT is about 3.08 ns, corresponding to the superconducting linac operating frequency 325 MHz. Comparing this spacing with the rotating period of hurling magnet field, typically on order of ms to sub-ms, the proton beam can be treated as a DC beam. In the rotating dipole magnetic field, the DC beam would be hurled, which is similar to a gentleman holding a brassie and hurling many golfs. Since then, the proton micro-bunches are arranged on target in the form of spiraling from inside to outside and then spiraling from outside to inside, again and again, making the beam footprints look like a spiral line, and to form similarly uniform distribution of the beam. So the magnet producing a rotating dipole magnetic field is called the hurling magnet.

A proper ratio between the amplitude modulation (AM) period T_1 and the field rotation period T_0 is critical to have a uniform distribution on target. The field rotation period T_0 $\left(T_0=\dfrac{2\pi}{\omega_0}\right)$ corresponds to the excitation current period of the sine-wave with amplitude modulation and contributes to space-uniformity distribution of the beam on target. To reduce sedimentary power in unit volume produced by proton beams passing a PBW and unbalanced thermal shock on a spallation target and nuclear fuel needles [5, 6], the lower limit 0.8 will be temporarily treated as a preliminary design data of the beam space uniformity on target. The AM period T_1 may be a time constant relating with mean generation time of neutrons on the MA transmuter and plays an important role in the beams time-uniformity. Since the mean generation time of neutrons in nuclear reactor is generally less than 1ms, T_1 is temporarily identified as 1 ms in the simulation process for the theoretical feasibility, which is basically in accord with the time of permitted proton "beam trip" mentioned in Ref. [7]. Maybe the value of T_1 will be revisited in the future. It seems, then, that the amplitude modulation frequency with kHz for the hurling magnet is much higher than that for conventional wobbler magnets. The new k-factor often used below is defined as $k=\dfrac{T_1}{T_0}$.

The hurling magnet designed similar to a sextupole magnet has three pairs of magnetic poles powered by three groups of the power respectively with the currents $I_1(t)\sin(\omega_0 t)$, $I_2(t)\sin\left(\omega_0 t-\dfrac{\pi}{3}\right)$ and $I_2(t)\sin\left(\omega_0 t+\dfrac{\pi}{3}\right)$. In case that the magnet yoke is not saturated, the magnetic field located in symmetric axis of this magnet can be expressed as

$$\begin{aligned}B_x(t;I_1,I_2,\omega_0) \propto\ & f(t)I_2\sin\left(\omega_0 t+\frac{\pi}{3}\right)\cos\left(+\frac{\pi}{6}\right)\\ & -f(t)I_2\sin\left(\omega_0 t-\frac{\pi}{3}\right)\cos\left(+\frac{\pi}{6}\right)\\ =\ & \frac{3I_2}{2}f(t)\cos(\omega_0 t),\end{aligned} \tag{2}$$

$$\begin{aligned}B_y(t;I_1,I_2,\omega_0) \propto\ & f(t)I_1\sin(\omega_0 t)\\ &+f(t)I_2\sin\left(\omega_0 t+\frac{\pi}{3}\right)\sin\left(+\frac{\pi}{6}\right)\\ &+f(t)I_2\sin\left(\omega_0 t-\frac{\pi}{3}\right)\sin\left(+\frac{\pi}{6}\right)\\ =\ & \left(I_1+\frac{I_2}{2}\right)f(t)\sin(\omega_0 t). \end{aligned} \tag{3}$$

In Eq. (2) and Eq. (3), $\frac{I_1}{I_2}$=constant and $f(t)$ is an AM function showed in Eq. (1), as shown in Fig. 1. The 3D model of the hurling magnet is given by 3D magnetic field simulation code OPERA in Fig. 2. During the simulation, the period of the rotating dipole magnetic field varying with time is 0.056 ms. When a single pair of magnetic pole is powered, the peak magnetic field is about 2400 Gs. Given the factors $\frac{3I_2}{2}$ and $I_1+\frac{I_2}{2}$, the maximum kick angle of the magnet for the 1.5 GeV proton beam in transverse directions is about 16.0 mrad corresponding to the maximum integrated field 0.120 Tesla-meter, which will be used in the following simulation.

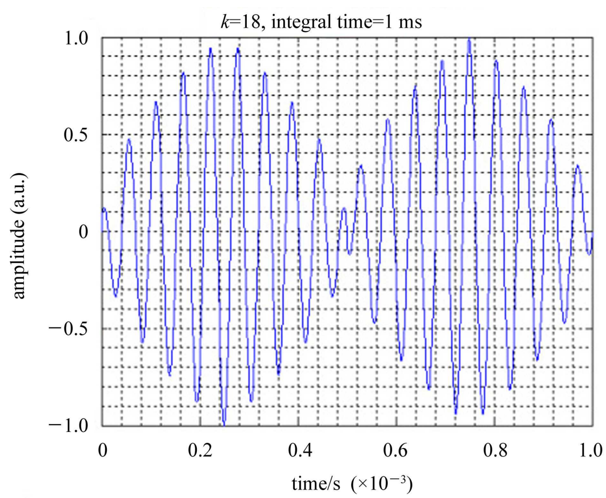

Fig. 1. The hurling field waveforms of the hurling magnet during 1 ms period. The value in the vertical axis is the amplitude normalized by the maximum amplitude.

However, the frequency of kHz for amplitude modulation brings some technical difficulties of magnet design and driving power supply and then the combination of various appropriate technologies may be needed. For this reason, the design of driving power supply with CW and high repetition frequency for the hurling magnet is a key technology for the design scheme of LTBT possibly developed soon. The development of some new technologies in recent years demonstrates that the inductive adding technique [18] with dozens of kHz or higher could be used for the system integration and assembling of high-power power supply, thereby improving the reliability of the power supply. Moreover, the parallel adding technique is also helpful for the excitation process of the hurling magnet (inductance value: several mH). And above all, it may be technically possible to construct an amplitude modulated and rotating dipole magnetic field (repetition frequency: more than ten kHz).

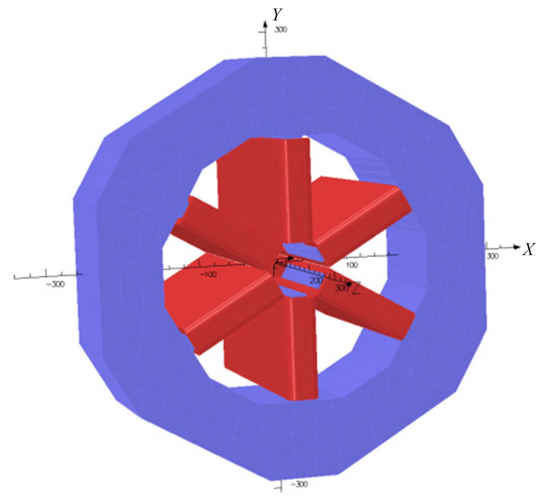

Fig. 2. The 3D sketch map of the hurling magnet. The size of the inner aperture is 64 mm and the pole face is simple at shape without optimization.

3 Distribution transformation by the hurling magnet

The uniformly distributed round beam with a 300 mm diameter could be achieved by the hurling magnet. To demonstrate the proton beam distribution transformation, the numerical simulation is carried out using 6.0×10^6 sampling protons during 1 ms. The Gaussian beam is conveniently adopted in simulation, even if the C-ADS linac may or may no provide a not very good Gaussian beam. The hurling magnet is regarded as a kick model of processing and then the (x'-y') phase space near the upstream and downstream of the hurling magnet is displayed in Fig. 3. Multi-particle simulation results of the transverse footprints on target corresponding to different k-factor and different beam sizes are shown in Fig. 3. In these figures, the color of the pixel in the right means the relative density, and the observation resolution is 100×100.

From Fig. 3, the approximately uniform distribution of the beam, through the hurling magnet, in the (x'-y') phase space is realized. Clearly, the beam distribution in this phase space well corresponds to the hurling waveform given in Fig. 1. As can be seen in Fig. 4, a large k-factor, meaning a small field rotation period T_0, can improve the beam uniformity on target. Furthermore, the uniformity of the beam spot core is proportional to the beam size coming from upstream of the hurling magnet, while the beam halo which can cause beam loss followed by excessive radioactivity will be increased by a large beam size. Moreover, the time average for the uniform distribution beam, namely the AM period T_1, should be as low as possible so that the distribution of sedimentary heat and neutrons on the PBW and the transmuter is not appreciably affected by the proton beams shift. However, the design of the hurling magnet and driving power supply with a high repetition frequency will face a challenge. So, a compromise would be needed for a practical design.

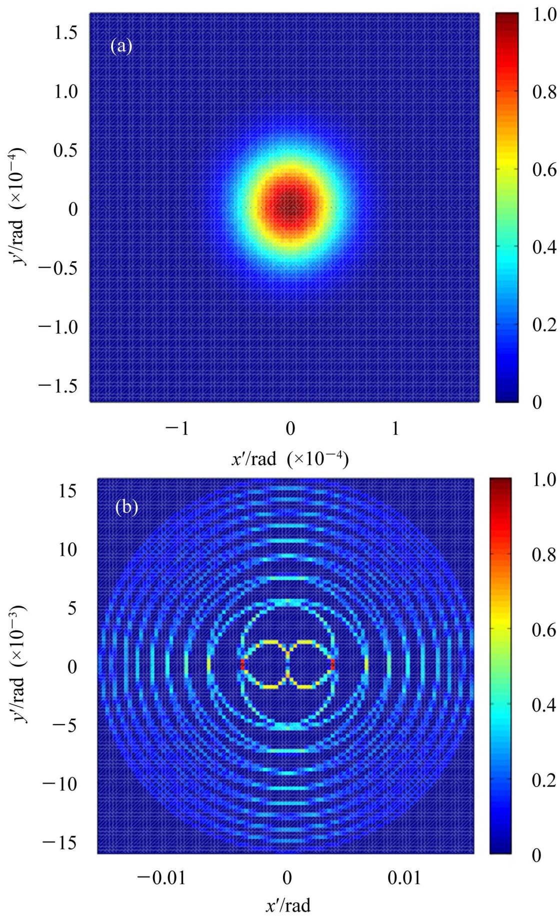

Fig. 3. The (x'-y') phase space: (a) near the upstream of the hurling magnet; (b) near the downstream of the hurling magnet. The input beam parameters are E = 1.5 GeV, k=18.0, $\sigma_{x,y}$ = 2.5 mm and $\epsilon_{N,x,y}$ = 0.45 πmm·mrad (r.m.s.). The maximum kicn transverse directions is about 16.0 mrad.

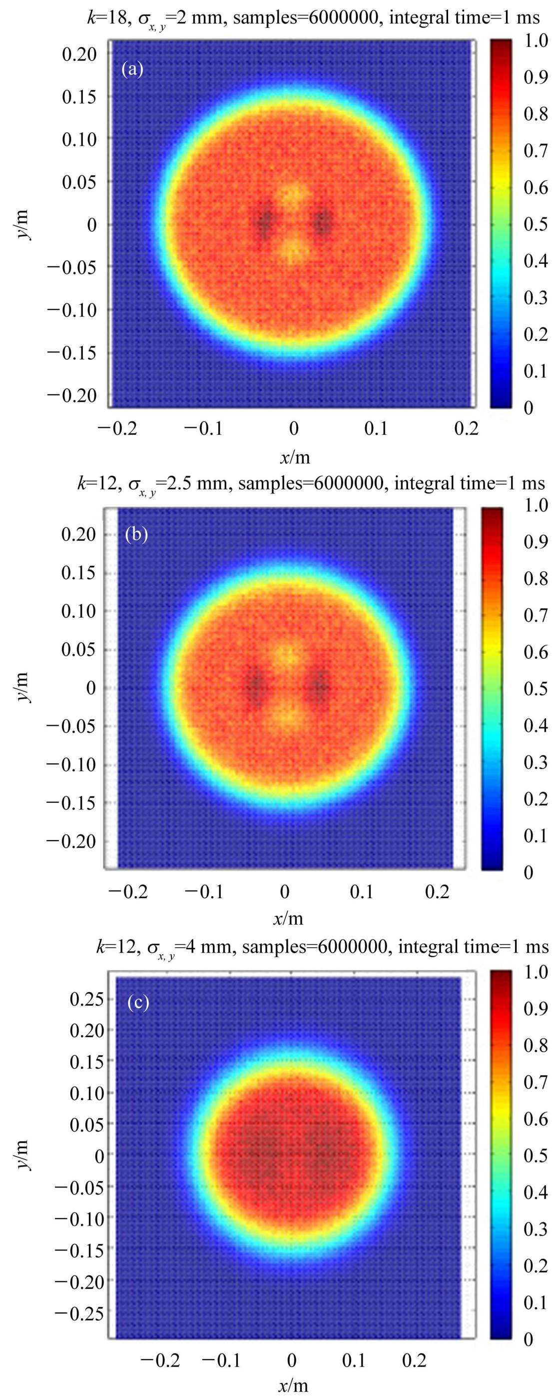

Fig. 4. Transverse distribution of the proton beam on target during 1 ms integrated time. The input beam parameters are: E=1.5 GeV, $\epsilon_{N,x,y}$=0.2 πmm·mrad (r.m.s.), (a) $\sigma_{x,y}$=2.0 mm (r.m.s.) and k=18; (b) $\sigma_{x,y}$=2.5 mm (r.m.s.) and k=12; (c) $\sigma_{x,y}$=4.0 mm (r.m.s.) and k=12.

4 The preliminary design of proton beam optics in C-ADS HTBT

The high current CW proton beam from the C-ADS linac has the specifications: $\sigma_{x,y}$ = 2.5 mm (r.m.s.) and $\epsilon_{N,x,y}$ = 0.2 π mm·mrad (r.m.s.). Gaussian beam will be adopted to implement simulation tracking. The beam footprint on target is a uniformly distributed round beam with a 300 mm diameter to be hopefully achieved in the simulation.

4.1 Design principle

LTBT probably includes several sections: a straight horizontal section starting from the linac exit, a horizontal bending section, a horizontal transport section starting from the hurling magnet, a vertical bending section and a vertical section. The section, connecting the C-ADS linac exit to the hurling magnet entrance, has a similar role to other general transport lines. So, the beam optics from the hurling magnet to transmuter beam transport section (HTBT) in C-ADS LTBT only will be discussed below. The overall layout of the C-ADS HTBT is shown in Fig. 5 (where the red elements represent a sequence of quadrupoles).

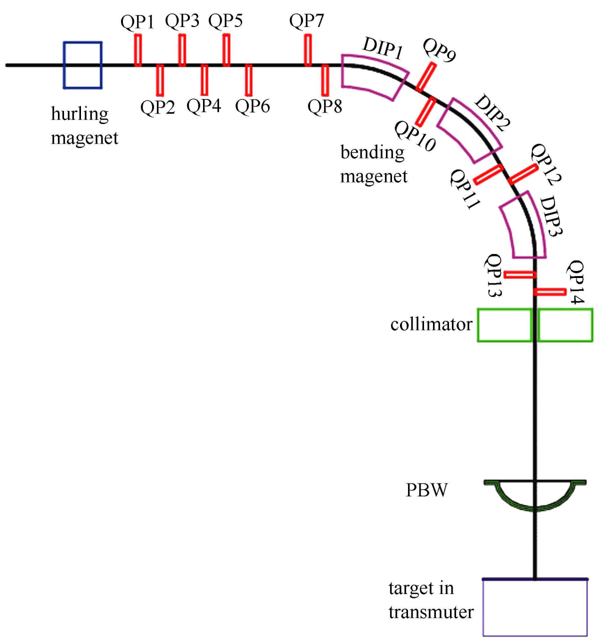

Fig. 5. The layout sketch of C-ADS HTBT. It is worth noting that the size proportion of individual elements and drift sections in this sketch is just schematic and may be different from the actual size.

The basic principle of the design scheme is as follows. As Fig. 5 shows, the beam coming from the upstream sections first passes through the hurling magnet, transforms to an approximately uniform distribution in the (x'-y') phase space, and then runs across a horizontal transport section to image at the front end of a vertical bending section. Soon afterwards, the beams traverse a vertical bending section and a vertical section including one collimators and one PBW, and then settle on a target. When $R_{x;2,1}=R_{y;2,1}$ in the thin-lens model is fulfilled by the transport matrix of C-ADS HTBT, the beam footprints with the approximate uniform distribution on target will be obtained.

For the horizontal transport section, the focusing imaging scheme is adopted. In the thin-lens model, the 6-quadrupole system is equivalent to a system composed of a thin-lens kick with identical horizontal and vertical focusing force f_{eff} and equivalent length L_{eff}. The hurling magnet is placed at $2f_{\text{eff}}$ upstream this virtual thin-lens kick and then the beam will be focused with the same or smaller transverse beam size at $2f_{\text{eff}}$ downstream this thin-lens kick. After then, the beam will enter the vertical bending section.

For the vertical bending section, a compact and achromatic TBA structure will be adopted. The 90-deg horizontal-to-vertical bending magnet system consists of three pieces of the same magnets with the magnetic field 1.5 T and the length 2.6 m. The same position double-waist on the vertical section is convenient for installing a collimator.

4.2 The beam optics design of C-ADS HTBT

As a preliminary design, an example of beam optics, including the horizontal transport section and the vertical bending section, appears in Fig. 6. The main parameters of individual elements are showed in Table 2. In Fig. 6, the length is 23.90 m with 6 quadrupoles system of 7.71 m. The equivalent length L_{eff} and equivalent focal length f_{eff} for the horizontal transport section are respectively 9.76 m and 2.72 m. The feature of dispersion function and amplitude functions are shown by the different color lines separately for the horizontal and vertical directions and the dispersion value at the end is 3.73×10^{-4} m.

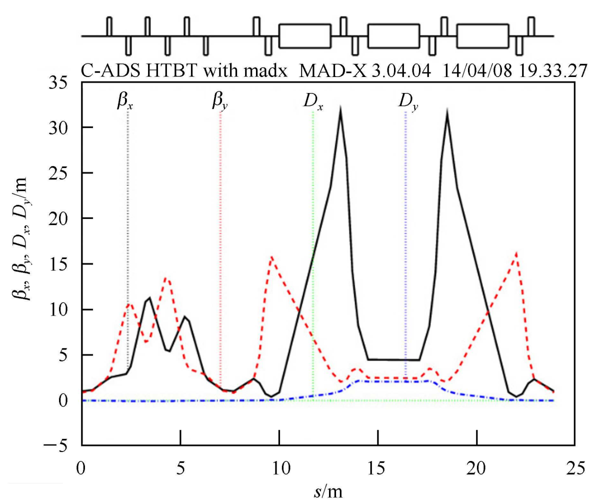

Fig. 6. The beta oscillation and dispersion function from the hurling magnet to the front end of a collimator.

The multi-particle simulations with k-factor 18 during 1 ms integrated time were implemented. The 1.5 GeV

Table 2. The parameters of main elements in C-ADS HTBT.

parameter name	parameter value	L/m
QP1/QP6	K/m^2 2.240/−2.240	0.200
QP2/QP5	K/m^2 −3.671/3.671	0.233
QP3/QP4	K/m^2 4.320/−4.320	0.212
QP7/QP14	K/m^2 5.820	0.300
QP8/QP13	K/m^2 −4.100	0.300
QP9/QP12	K/m^2 3.725	0.300
QP10/QP11	K/m^2 −3.200	0.300
DIP1/DIP2/DIP3	ρ/m 4.966	2.600

proton beam used for the simulation studies has the Gaussian distribution with the transverse normalized emittance 0.2 πmm·mrad (r.m.s.) and $\sigma_{x,y} = 2.5$ mm (r.m.s.). Nominal beam envelopes of the rms beam size (4 sigma) for the horizontal and vertical direction at two given time, meaning two given rotating dipole magnetic field in the hurling magnet, are illustrated in Fig. 7. The maximum footprint of beam transverse distributions at individual elements of C-ADS HTBT is given in Table 3. The maximum beam footprint on transverse directions is presented in the quadrupole QP12 showed in Fig. 5. The y axis of the DIP1 bending magnet gives the maximum gap of three bending magnets. As Fig. 8 shows, the closely uniformly distributed round beam on target is obviously achieved. It is worth mentioning that the particles of beam halo in the first subgraph of Fig. 8 may not be very ideal, but as a preliminary design scheme, this problem will be well improved, as beam optics will be further optimized and/or nonlinear magnets will be placed in front of the hurling magnet. The scheme of beam optics design for C-ADS HTBT may be slightly adjusted based on the practical engineering design, e.g., quadrupole.

Table 3. The transverse maximum of the beam footprint at different locations of C-ADS HTBT.

parameter	the Max. x/y	parameter	the Max. x/y
QP1	0.0328/0.0329	QP9	0.0779/0.0227
QP2	0.0344/0.0623	QP10	0.0435/0.0296
QP3	0.0602/0.0450	DIP2$_{\rm entr.}$	0.0280/0.0265
QP4	0.0372/0.0630	DIP2$_{\rm exit.}$	0.0360/0.0300
QP5	0.0515/0.0296	QP11	0.0544/0.0373
QP6	0.0278/0.0272	QP12	0.0974/0.0290
QP7	0.0301/0.0335	DIP3$_{\rm entr.}$	0.0779/0.0345
QP8	0.0137/0.0797	DIP3$_{\rm exit.}$	0.0138/0.0623
DIP1$_{\rm entr.}$	0.0167/0.0767	QP13	0.0138/0.0626
DIP1$_{\rm exit.}$	0.0715/0.0329	QP14	0.0251/0.0266

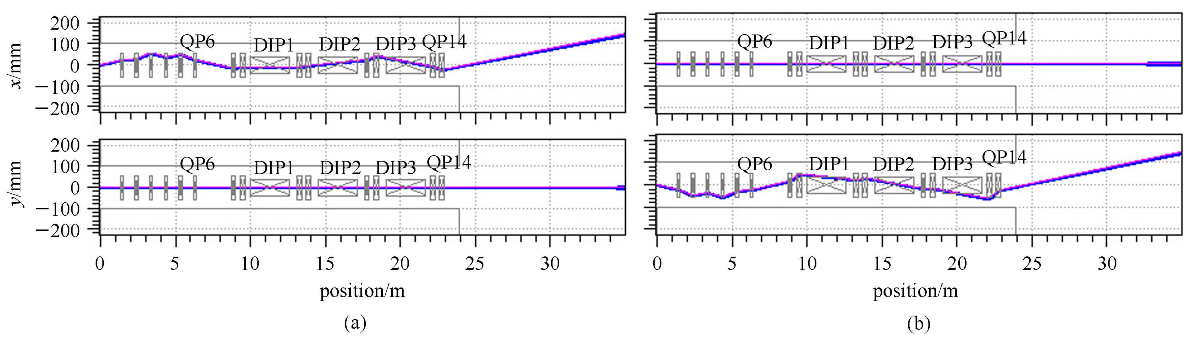

Fig. 7. The beam envelope of the rms beam size in C-ADS HTBT (4 sigma envelopes): (a) BL_x=0.0 Tesla-meter, BL_y=0.12 Tesla-meter; (b) BL_x=0.12 Tesla-meter, BL_y=0.0 Tesla-meter.

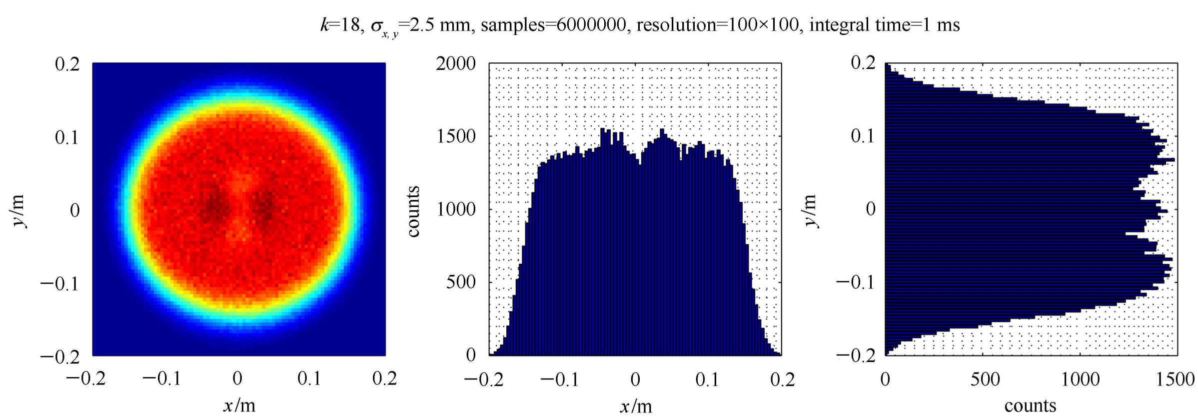

Fig. 8. Transverse distribution of the proton beam on target during 1 ms integrated time. The result showed in this figure is only a preliminary design value with a subsequent improvement of the design.

Corresponding to this beam optics, a beam double-waist at 10.43 m upstream the target is given in Fig. 9. At the double-waist point, the beam footprints for the two directions simultaneously have smaller values, and it is very convenient for installing a collimator with a 1.0 m length and a 15 mm inside radius to reduce the radiation damage caused by the back-scattering neutrons from the target.

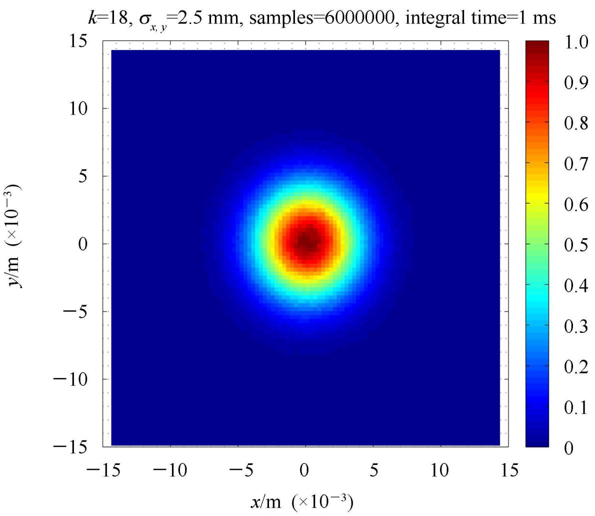

Fig. 9. The proton beam distribution at the double-waist point. The maximum of the beam footprint is 13.9/14.6 mm on the x/y axis.

Through the simulations and analyses above, one can realize that by choosing the suitable k-factor and beam size, a uniformly distributed round beam on target can be obtained by the combine of the hurling magnet, the focusing imaging scheme and the compact achromatic TBA structure, which primly meets the requirement of the space-time uniform feature of external neutron sources.

5 Summary

The distribution transformation of the beam by a rotating dipole magnetic field generated by the hurling magnet is studied. When the hurling magnet is driven by a more than ten kHz sine-wave current with a 1 kHz amplitude modulation, a uniformly distributed round beam with an about 300 mm diameter during a 1 ms in transverse directions is obtained for C-ADS, which is as a preliminary design data on target and maybe will be suitably adjusted in the future according to some further researches on the neutron dynamic of the transmuter. The beam optics, with the focusing imaging scheme and the compact achromatic TBA structure, of C-ADS HTBT is optimized for minimizing the beam loss. The double-waist point at 10.43 m upstream the target is convenient for installing a collimator to reduce the radiation damage caused by back-scattering neutrons.

References

1 Abderrahim H A, Galambosd J, Gohara Y et al. Fermilab-FN-0907-DI, 2010. 33
2 TANG J Y. Introduction to the China-ADS Project and Accelerator Design. In: FNAL Seminar, August 18, 2011
3 LI Z H. General Design of C-ADS Accelerator Physics. In: International Review Meeting on C-ADS Accelerator Physics Design, 19th-20th September, 2011
4 YAN Fang, LI Zhi-Hui. Physics Design on the Main Linac. In: International Review Meeting on C-ADS Accelerator Physics Design, 19th-20th September, 2011
5 Rubbia C, Rubio J A, Buono S et al. In: European Organization for Nuclear Research, CERN/AT/95-44 (ET), Geneva, 29th September, 1995
6 Cinotti L, Mansani L, Carluec B et al. In: Proceedings of the International Workshop on P&T and ADS Development, Framatome, SCK-CEN, Mol, Belgium, 6th-8th October, 2003
7 WENG W T, Ludewig H, Raparia D et al. In: Proceedings No. X Design of Proton Beam Optics to Realize Beam Distribution Transformation in C-ADS HTBT8 of 2011 Particle Accelerator Conference. New York, NY, USA, 2011. 4-6
8 Jean-Luc Biarrotte, Sebastien Bousson, Tomas Junquera et al. Nucl. Instrum. Mathods A, 2006, **562**: 656–661
9 TANG J Y, LI H H, AN S Z et al. Nucl. Instrum. Mathods A, 2004, **532**: 538–547
10 TANG J Y, WEI G H, ZHANG C. Nucl. Instrum. Mathods A, 2007, **582**: 326–335
11 Jason A J, Blind B. Beam Expansion with Speciednal Distribution. In: Proceedings of 1997 Particle Accelerator Conference, Vancouver, B. C., Canada, 1997. 3728–3730
12 JIA Xian-Lu, ZHANG Tian-Jue, LÜ Yin-Long et al. High Energy Physics and Nuclear Physics, 2007, **31**(3): 292–295 (in Chinese)
13 REN Xiu-Yan, LU Yu-Zhu. Atomic Energy Science and Technology, 2011, **45**(7): 868–871 (in Chinese)
14 CHU W T, Curtis S B, Llacer J et al. IEEE Transactions on Nuclear Science, 1985, **32**(5): 3321–3323
15 Terakawa A, Ishii K, Okamura H. Design of the Rotating Beam-Irradiation System Employing the Beam Swinger for Charged-Particle Therapy Experiments at CYRIC, In: CYRIC Annual Report 2003.40–42
16 Komori M, Furukawa T et al. Design of Compact Irradiation Port for Carbon Radiotheraphy Facility. In: Proceedings of APAC 2004, Gyeongju, Kerea, 2004. 417–419
17 Shunsuke Yonai, Nobuyuki Kanematsu, Masataka Komori et al. Med. Phys., 2008, **35**(3): 927–938
18 XU Yu-Cun, WANG Xiang-Qi, FENG De-Ren et al. High Power Laser and Particle Beams, 2008, **20**(6): 1043–1047 (in Chinese)